Volume 306 issues 1–3, 1 October 2007   ISSN 0927-7757

ELSEVIER

COLLOIDS AND SURFACES

An International Journal

PHYSICOCHEMICAL AND ENGINEERING ASPECTS

www.elsevier.com/locate/colsurfa

Adsorption of organic acids on metal oxides: Application of the surface potential measurements

Nikola Kallay *, Tajana Preočanin, Jelena Marković, Davor Kovačević

*Laboratory of Physical Chemistry, Department of Chemistry, Faculty of Science, University of Zagreb,
Horvatovac 102a, 10000 Zagreb, Croatia*

Abstract

Simultaneous interpretation of surface potential, electrokinetic and adsorption data for salicylic acid on hematite surface was introduced. The interpretation on the basis of the surface complexation model using both 2-pK and 1-pK models suggested that salicylate ion is bound to one metal ion at the solid surface by two oxygen bonds. The equilibrium parameters describing the interfacial equilibrium were obtained as follows: for the 2-pK model the thermodynamic equilibrium constant for protonation and deprotonation of surface sites are lg $K_p^0 = 4.1 \pm 0.2$ and lg $K_d^0 = -8.2 \pm 0.2$, respectively, while the thermodynamic equilibrium constant of adsorption of salicylic acid is $lg\ K_{a1}^0 = 1.6 \pm 0.1$. For 1-p$K$ model the thermodynamic equilibrium constant of adsorption of salicylic acid was obtained as lg $K_{a3}^0 = 2.3 \pm 0.2$. The inner layer capacitance increases with pH from 1.8 to 3 F m^{-2}. It was shown that the surface potential measurement by single crystal electrodes is a helpful tool in elucidation of the complex equilibrium at the interface.

1. Introduction

Adsorption of organic ionic species on metal oxides is a subject of numerous publications [1–21]. One of the reasons for the extensive research in this field is related to the environmental problems since the organic pollutants adsorb on metal oxides in the soil. They undergo dissociation in the bulk of the liquid medium, which should also be taken into account. In the case of the reversibility, the adsorption/desorption kinetics and equilibrium govern their transport in the soil. Adsorption equilibrium of ionic species is markedly influenced by the electrostatic potential at the solid/liquid interface. Most of the experimental findings concern adsorption isotherms as a function of pH and are often accompanied by electrokinetic data. The interpretation is sometimes semi quantitatively based on the Langmuir isotherm [22], while more detailed studies are based on the surface complexation model (SCM) in the original form [23] and on the more advanced MUSIC model [24]. The application of SCM requires

the choice of the reaction mechanism, i.e. the knowledge of the conformation of the surface complex. However, the adsorption data solely do not suffice to distinguish between different hypotheses. For example, several different conformations of salicylic ions adsorbed at metal oxide surface were proposed on the basis of spectroscopy and adsorption data [6,7,12–17,20,21]. It is clear that the problem might be solved by introducing a new experimental technique. Recently, the measurements of the surface potential by means of the single crystal electrodes were introduced [25]. Surface potential φ_0, as evaluated from the potential of the single crystal electrode, corresponds to the electrostatic potentials of the inner plane of the electric interfacial layer (EIL). This potential affects directly the state of ionic species created by interactions with potential determining ions and bound directly to the solid surface. Other ions may be either associated to these surface charges or bound directly to the surface. The aim of this study is to apply surface potential measurements in order to elucidate the adsorption mechanism of organic species and to evaluate corresponding equilibrium parameters. For this purpose salicylic acid and hematite will be used as a model system. Our previous report on this subject was based on the adsorption and electrokinetic data [10]. This arti-

* Corresponding author. Tel.: +385 1 4606 133; fax: +385 1 4606 131.
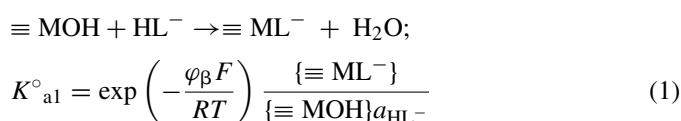*E-mail address:* nkallay@chem.pmf.hr (N. Kallay).

cle uses reported data, but introduces new results on the surface potentials for the same system.

2. Theory

The interpretation of data will be based on the model of electrical interfacial layer [26] and on the surface complexation model [23] assuming both 2-pK and 1-pK mechanisms. Within the EIL, several layers and planes are postulated. The first plane at the solid surface (0-plane) is characterized by inner surface potential φ_0. Centers of associated counterions are located in the β-plane and are characterized by the outer surface potential φ_β. The specifically adsorbed organic ions might be located either in 0-plane or in β-plane. In some cases one is forced to postulate a new plane in which organic ionic surface species are located. The onset of diffuse layer is d-plane with electrostatic potential φ_d. Diffuse layer may be divided in two parts, the immobile one that stays (or moves) together with solid surface (so-called hydrodynamically stagnant layer) and the mobile one that moves (or stays) together with the bulk of the liquid medium. These two parts of the diffuse layer are divided by the hydrodynamic slip or shear plane (s-plane) characterized by the electrokinetic ζ-potential. Within the double layer approximation (DL), which is in fact the basic stern model, the onset of diffuse layer is taken as β-plane so that $\varphi_d = \varphi_\beta$, while the triple layer model (TLM) assumes significant potential drop between β- and d-planes [26,27].

For the interpretation of data on the basis of the surface complexation model one should consider conformation of salicylic species at the metal oxide surface. At first, the formation of complex with one surface metal ion will be considered [1,9,11,12,15]. In the pH range covered by the experiment the dominant salicylate species in the bulk of the solution are singly charged HL$^-$ ions, so that formation of the surface complex may be described as binding of these species to active surface sites.
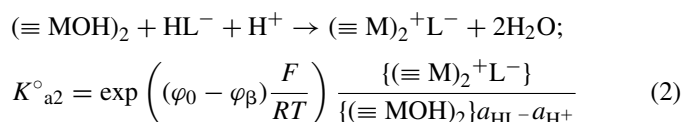
In view of the 2-pK mechanism binding of salicylate ions should be considered as interactions with amphoteric ≡MOH sites:

$$\equiv MOH + HL^- \rightarrow \equiv ML^- + H_2O;$$

$$K^{\circ}_{a1} = \exp\left(-\frac{\varphi_\beta F}{RT}\right)\frac{\{\equiv ML^-\}}{\{\equiv MOH\}a_{HL^-}} \quad (1)$$

where ≡MOH stands for the hydrated metal atom at the surface, ≡ML$^-$ is the surface complex, K°_{a1} is the thermodynamic surface equilibrium constant of the reaction (1), curly brace denotes surface concentration of defined surface species, and φ_β is the electrostatic potential affecting the state of salicylate ions at the surface. The above mechanism will be later in the text denoted as mechanism (1). As it will be discussed later, the exponential term represents the activity coefficients [28]. Regarding the water molecules, in considering the equilibrium it does not make any difference if they are in the hydration shell at the interface or released from the surface, as denoted in the above equation. If one writes the reaction equation as binding of uncharged H$_2$L molecules, or doubly charged L^{2-} ions, the equilibrium equations will be equivalent and the corresponding

equilibrium constants will be simply related through the acid dissociation equilibrium constants in the bulk of the solution. The same applies if one introduces positive surface sites ≡MOH$_2^+$ instead of the neutral sites ≡MOH. In considering the equilibrium, the conformation of the resulting product is of the main importance. Also, the equilibrium Eq. (1) applies for both mono and bidentate complex.
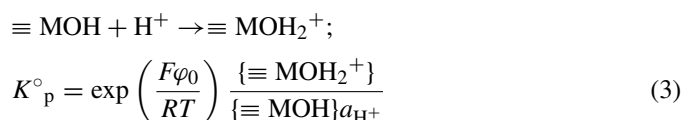
Another possibility, that is interesting to examine, is the formation of uncharged bidentate complex with two neighboring surface metal ions [1,9,12,15]:
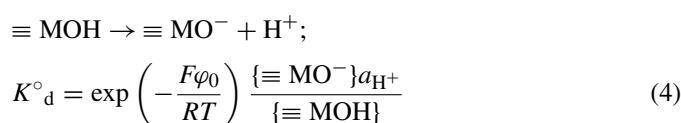
$$(\equiv MOH)_2 + HL^- + H^+ \rightarrow (\equiv M)_2{}^+L^- + 2H_2O;$$

$$K^{\circ}_{a2} = \exp\left((\varphi_0 - \varphi_\beta)\frac{F}{RT}\right)\frac{\{(\equiv M)_2{}^+L^-\}}{\{(\equiv MOH)_2\}a_{HL^-}a_{H^+}} \quad (2)$$

Note that (≡MOH)$_2$ stands for two sites that are already together, while 2(≡MOH) would mean two independent sites. In the expression for equilibrium constant the latter case would require introduction of the square of surface concentration {≡MOH}.

According to (2) a charge separation takes place within the surface complex affecting the activity coefficient of the surface complex. The above mechanism will be later in the text denoted as mechanism (2). Regarding the charge separation within the surface complex, other possibilities were also examined and will be considered in the discussion part of the article.

Assuming 2-pK mechanism [29] of surface charging, due to interactions of metal oxide surface with potential determining H$^+$ and OH$^-$ ions, the following relationships hold:

$$\equiv MOH + H^+ \rightarrow \equiv MOH_2{}^+;$$

$$K^{\circ}_p = \exp\left(\frac{F\varphi_0}{RT}\right)\frac{\{\equiv MOH_2{}^+\}}{\{\equiv MOH\}a_{H^+}} \quad (3)$$

and

$$\equiv MOH \rightarrow \equiv MO^- + H^+;$$

$$K^{\circ}_d = \exp\left(-\frac{F\varphi_0}{RT}\right)\frac{\{\equiv MO^-\}a_{H^+}}{\{\equiv MOH\}} \quad (4)$$

where K°_p and K°_d are thermodynamic equilibrium constants of protonation and deprotonation of amphoteric surface ≡MOH sites, respectively, while φ_0 is the inner surface potential, i.e. the electrostatic potential affecting the state of charged surface groups ≡MOH$_2^+$ and ≡MO$^-$.

The concept of standard states at the interface enables definition of the activity coefficients of surface species [28] and thus exact treatment of the equilibrium. For complex species, with several charged groups exposed to different electrostatic potentials, the following relationship holds:

$$RT \ln \gamma_S = \sum_i z_i \varphi_i F \quad (5)$$

where z_i is the charge number of i-th ionic group (exposed to electrostatic potential φ_i) composing the surface complex S. Accordingly, activity coefficients for already defined surface

species are defined as follows:

$$\gamma(\equiv \mathrm{MOH_2^+}) = \exp\left(\frac{\varphi_0 F}{RT}\right) \tag{6}$$

$$\gamma(\equiv \mathrm{MO^-}) = \exp\left(-\frac{\varphi_0 F}{RT}\right) \tag{7}$$

$$\gamma(\equiv \mathrm{ML^-}) = \exp\left(-\frac{\varphi_\beta F}{RT}\right) \tag{8}$$

$$\gamma((\equiv \mathrm{M})_2{}^+\mathrm{L^-}) = \exp\left((\varphi_0 - \varphi_\beta)\frac{F}{RT}\right) \tag{9}$$

Introduction of activity coefficients, defined by relations (6–9), resulted in equilibrium Eqs. (1)–(4).

The definition of the total surface concentration of active surface sites Γ_{tot} depends on the assumed conformation of salicylate surface complex, so that for mechanisms (1) and (2):

$$\Gamma_{\mathrm{tot}} = \{\equiv \mathrm{MOH}\} + \{\equiv \mathrm{MOH_2^+}\} + \{\equiv \mathrm{MO^-}\} + \Gamma_{\mathrm{L}};$$

$$\text{mechanism (1)} \tag{10}$$

$$\Gamma_{\mathrm{tot}} = \{\equiv \mathrm{MOH}\} + \{\equiv \mathrm{MOH_2^+}\} + \{\equiv \mathrm{MO^-}\} + 2\Gamma_{\mathrm{L}};$$

$$\text{mechanism (2)} \tag{11}$$

where Γ_{L} denotes surface concentration of salicylate species regardless to their conformation at the surface.

The definition of the net or effective surface charge density σ_{s} also depends on the assumed reaction mechanisms (1 or 2). It is equal in magnitude but opposite in sign with respect to the "surface charge density of the diffuse layer" σ_{d}:

$$\sigma_{\mathrm{s}} = -\sigma_{\mathrm{d}} = F(\{\equiv \mathrm{MOH_2^+}\} - \{\equiv \mathrm{MO^-}\} - \Gamma_{\mathrm{L}});$$

$$\text{mechanism (1)} \tag{12}$$

$$\sigma_{\mathrm{s}} = -\sigma_{\mathrm{d}} = F(\{\equiv \mathrm{MOH_2^+}\} - \{\equiv \mathrm{MO^-}\}); \quad \text{mechanism (2)} \tag{13}$$

According to the Gouy–Chapman theory, the net surface charge density is related to the potential at the onset of diffuse layer φ_{d} by

$$\sigma_{\mathrm{s}} = -\sigma_{\mathrm{d}} = -\sqrt{8RT\varepsilon I_{\mathrm{c}}}\ \sinh\left(\frac{F\varphi_{\mathrm{d}}}{2RT}\right) \tag{14}$$

where I_{c} is the ionic strength and ε the permittivity of the medium.

The relationship between φ_{d} and electrokinetic ζ-potential is given by the same theory as

$$\varphi_{\mathrm{d}} = \frac{2RT}{F}\ \ln\left(\frac{\exp(-\kappa s) + \mathrm{th}(F\zeta/4RT)}{\exp(-\kappa s) - \mathrm{th}(F\zeta/4RT)}\right) \tag{15}$$

where s is the separation distance of the electrokinetic s-plane from the d-plane, and κ is the Debye–Hückel parameter given by

$$\kappa = \sqrt{\frac{2I_{\mathrm{c}}F^2}{\varepsilon RT}} \tag{16}$$

The definition of the surface charge density in 0-plane (σ_0) also depends on the assumed mechanism, (1) and (2), respectively

$$\sigma_0 = F(\{\equiv \mathrm{MOH_2^+}\} - \{\equiv \mathrm{MO^-}\}); \quad \text{mechanism (1)} \tag{17}$$

$$\sigma_0 = F(\{\equiv \mathrm{MOH_2^+}\} - \{\equiv \mathrm{MO^-}\} + \Gamma_{\mathrm{L}}); \quad \text{mechanism (2)} \tag{18}$$

The above equations assume that negatively charged salicylate ions are not directly bound to the surface and that they have markedly higher adsorption affinity than other anions in the solution, i.e. than $\mathrm{NO_3^-}$ ions.

The capacitance of the inner layer capacitor C_1 is commonly defined by

$$C_1 = \frac{\sigma_0}{\varphi_0 - \varphi_\beta} \tag{19}$$

Eqs. (3) and (4) yield the expression for the surface potential in 0-plane as

$$\varphi_0 = \frac{RT \ln 10}{F}\left(\frac{1}{2}\ \mathrm{lg}\ \frac{K^\circ_{\mathrm{p}}}{K^\circ_{\mathrm{d}}} - \mathrm{pH}\right)$$

$$- \frac{RT \ln 10}{2F}\ \mathrm{lg}\left(\frac{\{\equiv \mathrm{MOH_2^+}\}}{\{\equiv \mathrm{MO^-}\}}\right) \tag{20}$$

According to above equation the electroneutrality point [30], or the pristine point of zero charge [31,32], $\mathrm{pH_{eln}}$, at which all electrical properties diminish, $\{\equiv \mathrm{MOH_2^+}\} = \{\equiv \mathrm{MO^-}\}$ and ($\varphi_0 = 0$), is given by
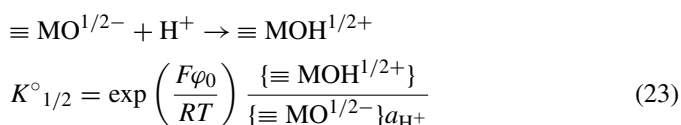
$$\mathrm{pH_{eln}} = \frac{1}{2}\ \mathrm{lg}\ \frac{K^\circ_{\mathrm{p}}}{K^\circ_{\mathrm{d}}} \tag{21}$$

so that

$$\varphi_0 = \frac{RT \ln 10}{F}(\mathrm{pH_{eln}} - \mathrm{pH}) - \frac{RT}{2F}\ \ln\left(\frac{\{\equiv \mathrm{MOH_2^+}\}}{\{\equiv \mathrm{MO^-}\}}\right) \tag{22}$$

The first term in Eq. (22) is Nernstian, while the second one determines a decrease in the slope with respect to the Nernstian enabling evaluation of the ratio of concentrations of positive and negative surface groups. In the absence of specific adsorption and in the case of negligible or symmetric ionic association, the electrokinetic isoelectric point ($\mathrm{pH_{iep}}$), the point of zero charge ($\mathrm{pH_{pzc}}$), and the point of zero potential ($\mathrm{pH_{pzp}}$), coincide with $\mathrm{pH_{eln}}$.

Adsorption of salicylate ions ($\mathrm{HL^-}$) at metal oxide surface could be also interpreted on the basis of 1-pK mechanism of surface charging:

$$\equiv \mathrm{MO^{1/2-}} + \mathrm{H^+} \rightarrow\ \equiv \mathrm{MOH^{1/2+}}$$

$$K^\circ_{1/2} = \exp\left(\frac{F\varphi_0}{RT}\right)\frac{\{\equiv \mathrm{MOH^{1/2+}}\}}{\{\equiv \mathrm{MO^{1/2-}}\}a_{\mathrm{H^+}}} \tag{23}$$

The formation of the salicylate surface complex with metal atom is then described as

$$\equiv MO^{1/2+} + HL^- \rightarrow \equiv M^{1/2+}L^- + H_2O$$

$$K^{\circ}_{a3} = \exp\left(-\frac{F\varphi_\beta}{RT}\right)\frac{\{\equiv M^{1/2+}L^-\}}{\{\equiv MOH^{1/2+}\}a_{HL^-}} \tag{24}$$
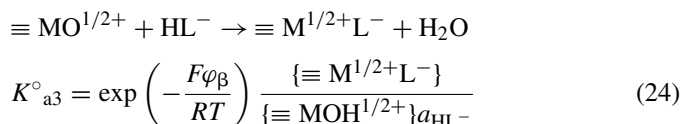
The equivalent relationship could be obtained if binding with negative $\equiv MO^{1/2-}$ sites is assumed, and also if binding of H_2L or L^{2-} is considered. The only assumption of importance is the conformation of the surface complex $\equiv M^{1/2+}L^-$. Eq. (24) applies for the surface complex in which the charge on metal remains +1/2.

In principle, it is possible to speculate that the metal in the surface complex is uncharged, i.e. that surface complex is $\equiv M^0 L^{1/2-}$. Another problem is the electrostatic potential affecting different parts of the surface complex. Eq. (24) is based on the assumption that metal is exposed to the surface potential φ_0, while the ligands are affected by the potential φ_β. In this article we shall also examine the possibility that both metal and ligand are exposed to the surface potential φ_0. The exponential term in the Eq. (24) is the ratio of the activity coefficients of the surface species. According to (5) the activity coefficients are as follows

$$\gamma(\equiv MO^{1/2-}) = \exp\left(\frac{-0.5\varphi_0 F}{RT}\right) \tag{25}$$

$$\gamma(\equiv MOH^{1/2+}) = \exp\left(\frac{0.5\varphi_0 F}{RT}\right) \tag{26}$$

$$\gamma(\equiv M^{1/2+}L^-) = \exp\left((0.5\varphi_0 - \varphi_\beta)\frac{F}{RT}\right) \tag{27}$$

Once the activity coefficients are defined, one could introduce them in the equilibrium equation and obtain the exponential term in the equilibrium equation.

According to Eq. (23) the surface potential for 1-pK mechanism is equal to

$$\varphi_0 = \frac{RT \ln 10}{F}(\lg^0_{1/2} - pH) - \frac{RT}{F}\ln\left(\frac{\{\equiv MOH^{1/2+}\}}{\{\equiv MO^{1/2-}\}}\right) \tag{28}$$

The thermodynamic equilibrium constant of protonation is given by

$$\lg K^{\circ}_{1/2} = pH_{eln} \tag{29}$$

3. Experimental

3.1. Materials

All solutions were prepared using redistilled and decarbonised water: $NaNO_3$ (*p.a.*, Fluka), HNO_3 (0.1 mol dm^{-3}, titrival, Fluka), NaOH (0.1 mol dm^{-3}, titrival, Fluka), standard buffers (Fluka), NaOH (0.1 mol dm^{-3}, titrival, Fluka), salicylic acid (*p.a.*, Fluka), standard buffers (Fluka). The hematite single crystal electrode was prepared using mineral sample from Vesuvius (Italy) and is shown in Fig. 1.
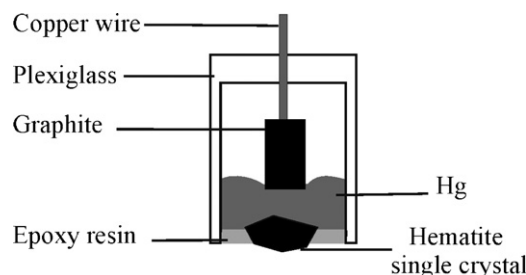

Fig. 1. Hematite single crystal electrode.

3.2. Methods

Surface potential of hematite was measured by hematite single crystal electrode as a function of pH, which was varied by NaOH and HNO_3. The experiments were performed in the presence and in the absence of salicylic acid. Electrode potential of hematite electrode was measured using the Methrom 827 pH-meter. The pH was measured with glass electrode (Metrohm, 6.0222.100) using a separate Methrom 827 pH-meter. Reference electrode was Ag/AgCl/Cl$^-$ with salt bridge (Metrohm, 6.0233.100) filled with same electrolyte solution as in the measuring system. The glass electrode was calibrated with three standard buffers. In the course of measurements the system was thermostated at 25.0 °C and kept under an argon atmosphere. The surface potentials were evaluated from the measured hematite electrode potentials by calibration in absence of salicylic acid at low ionic strength. The isoelectric point, as measured by electrophoresis of suspended hematite particles at low ionic strength of 1×10^{-3} mol dm^{-3} (pH$_{iep}$ = 6.2), was taken as the pristine point of zero charge pH$_{eln}$ and thus as the point of zero potential for that condition. It was found [33] that surface potential of hematite in nitric acid aqueous solution ($I_c = 10^{-2}$ mol dm^{-3}, pH = 4.2) is $\varphi_0 = 47$ mV. The electrode potential of single crystal hematite electrode in the same conditions was found to be $E = -50$ mV. Therefore the surface potentials were calculated from electrode potentials by adding 97 mV. The procedure is described in more details in previous reports [30,33]. Adsorption and electrokinetic data were taken from our previous publication [10].

4. Interpretation

The data were interpreted by using the surface complexation model. Surface potential data enabled us to avoid the linear regression analysis based on the assumption of the constancy of equilibrium parameters. Instead, in our calculations equilibrium parameters K°_p, K°_d, K°_{a1} and K°_{a2} (in the case of 2-pK model), K°_{a3} (in the case of 1-pK model), as well as the capacitance C_1 (for both models) were calculated from each measurement point. In doing so, the corresponding values of Γ_L and ζ were obtained by interpolation of experimental data. In the calculations, the value of s was assumed as 10 Å. In the case of 2-pK mechanism it was necessary to assume also the value of Γ_{tot}. The effect of these assumptions will be discussed later. Such an approach based on simultaneous interpretation of
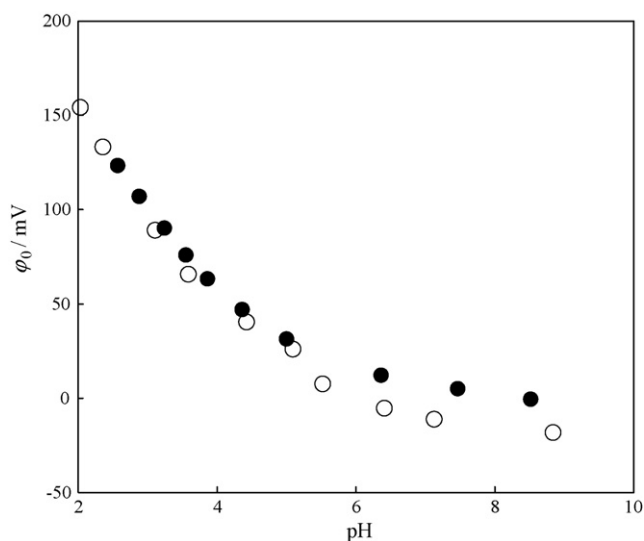
Fig. 2. Surface potential of hematite (φ_0) as a function of pH at 25 °C in absence (○) and in the presence (●) of salicylic acid (7.21×10^{-3} mol dm^{-3}). Ionic strength was adjusted with NaNO$_3$; $I_c = 1.6 \times 10^{-2}$ mol dm^{-3}.

sets of measured data (φ_0, ζ and Γ_L, Figs. 2–4) enables a test of the constancy of equilibrium parameters for examined pH range, and thus critical evaluation of the proposed adsorption mechanisms.

4.1. The procedure for 2-pK mechanism is as follows

4.1.1. Calculation of thermodynamic equilibrium constants of surface protonation and deprotonation

(i) Calculation of φ_d from measured electrokinetic ζ-potentials using Eqs. (15) and (16) assuming $s = 10$ Å. The calcula-
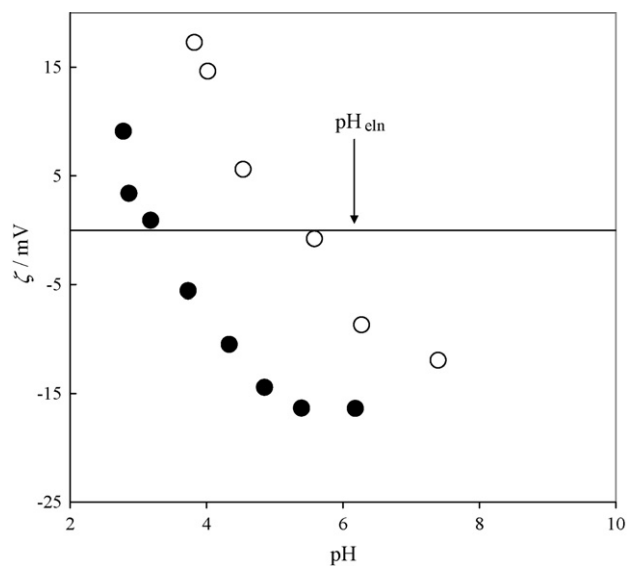

Fig. 3. Electrokinetic ζ-potential of hematite as a function of pH at 25 °C in absence (○) and in the presence (●) of salicylic acid (7.21×10^{-3} mol dm^{-3}) taken from Ref. [10]. Ionic strength was adjusted with NaNO$_3$; $I_c = 1.6 \times 10^{-2}$ mol dm^{-3}. The pristine point of zero charge pH$_{eln} = 6.2$ is denoted by an arrow. Reproduced with permission from Croatica Chemica Acta.
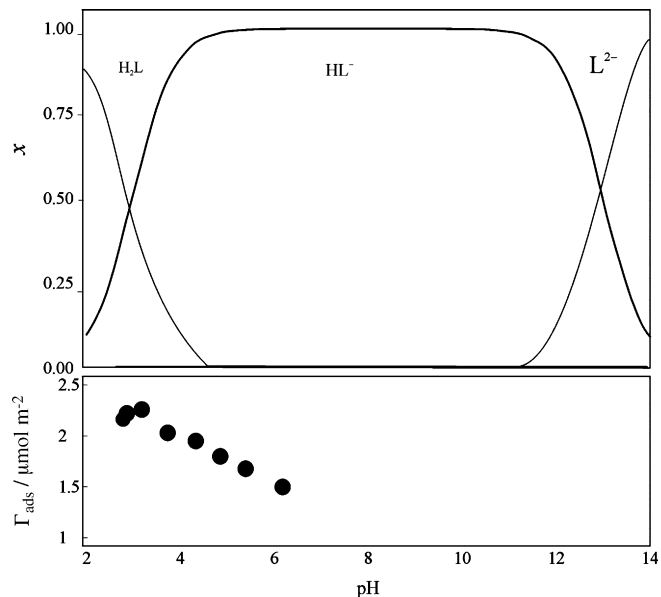

Fig. 4. Upper part: speciation of the salicylic acid in the bulk of the solution. In the calculations the following values of the dissociation equilibrium constants were used [38] $K_1 = 1.06 \times 10^{-3}$ mol dm^{-3}; $K_2 = 1 \times 10^{-13}$ mol dm^{-3}. Lower part: surface concentration of salicylate species at the hematite surface (●) as a function of pH at 25 °C taken from Ref. [10]. Total equilibrium bulk concentration of salicylic acid was 7.21×10^{-3} mol dm^{-3}. Ionic strength was adjusted with NaNO$_3$; $I_c = 1.6 \times 10^{-2}$ mol dm^{-3}. Reproduced with permission from Croatica Chemica Acta.

tions were repeated for a broad range of s values, from 0 to 20 Å, but the effect of the choice of the s-value was not significant.

(ii) Calculation of σ_s from φ_d (obtained in step i) using Eq. (14).

(iii) Evaluation of the ratio $\{\equiv MOH_2^+\}/\{\equiv MO^-\}$ from surface potential data using Eq. (22) taking pH$_{eln} = 6.2$, corresponding to pH$_{iep}$ measured in absence of salicylic acid at low ionic strength of 1×10^{-3} mol dm^{-3}.

(iv) Calculation of the individual values of $\{\equiv MOH_2^+\}$ and $\{\equiv MO^-\}$ from their ratio (obtained in step iii) using calculated σ_s (obtained in step ii) and measured Γ_L values. For mechanisms (1) and (2), Eqs. (12) and (13) were used, respectively.

(v) Calculation of surface concentration of neutral $\{\equiv MOH\}$ sites from $\{\equiv MOH_2^+\}$ and $\{\equiv MO^-\}$ values (obtained in step iv) and measured Γ_L values, assuming $\Gamma_{tot} = 1.5 \times 10^{-5}$ mol m^{-2}. For mechanisms (1) and (2), Eqs. (10) and (11) were used, respectively. The results were sensitive on the choice of Γ_{tot} value so the calculations were repeated for the values of Γ_{tot} in the range of $1–5 \times 10^{-5}$ mol m^{-2}.

(vi) Once all surface concentrations are known (as obtained in steps iv and v) one uses Eqs. (3) and (4) and calculates K°_p and K°_d values using the experimental values of φ_0. The results were sensitive on the $\{\equiv MOH\}$ values (obtained in step v), i.e. on the choice of Γ_{tot} value. Therefore the calculations were repeated for the values of Γ_{tot} in the range of $1–5 \times 10^{-5}$ mol m^{-2}. As expected, the ratio K°_p/K°_d yielded pH$_{eln} = 6.2$ for all pH values (Eq.

N. Kallay et al. / Colloids and Surfaces A: Physicochem. Eng. Aspects 306 (2007) 40–48

45
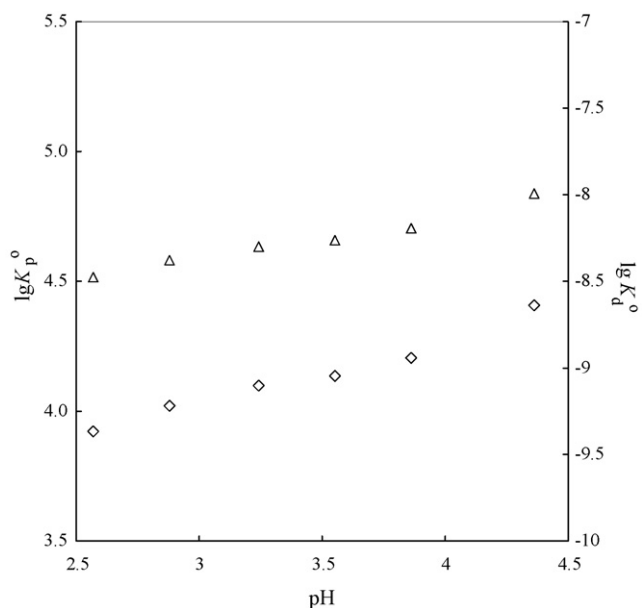
Fig. 5. Thermodynamic equilibrium constant of surface protonation K°_p ($\diamond$) and deprotonation K°_d ($\triangle$) of amphoteric hematite surface sites, as calculated for 2-pK model (mechanism 1) using experimental data shown in Figs. 2–4; $I_c = 1.6 \times 10^{-2}$ mol dm^{-3}, $t = 25\,^\circ$C. Assumed values: $\Gamma_{tot} = 1.5 \times 10^{-5}$ mol m^{-2}; $s = 10$ Å.
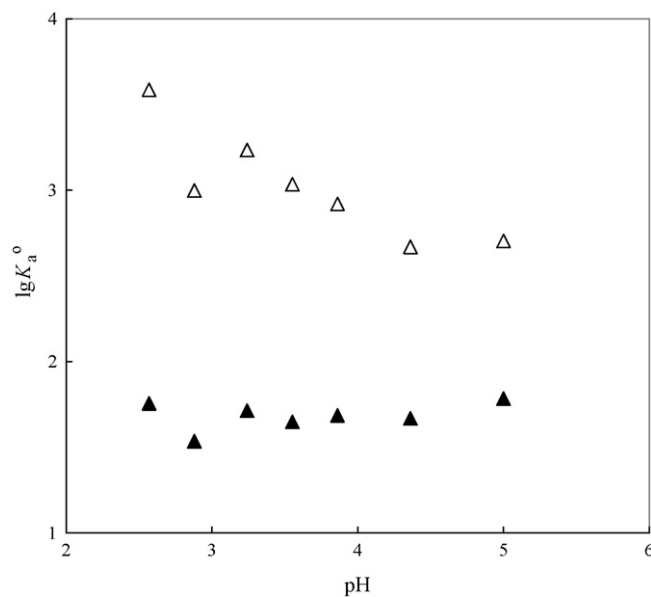

Fig. 6. Thermodynamic equilibrium constant of adsorption of salicylic acid at hematite, as calculated for 2-pK model (mechanism 1) using experimental data shown in Figs. 2–4; $I_c = 1.6 \times 10^{-2}$ mol dm^{-3}, $t = 25\,^\circ$C. Assumed values: $\Gamma_{tot} = 1.5 \times 10^{-5}$ mol m^{-2}; $s = 10$ Å. In calculations different internal charge distributions within the surface complex were assumed: K°_{a1} ($\equiv$ML$^-$) ($\blacktriangle$) and K°_{a2} ($\equiv$M$^+$L^{2-}) ($\triangle$).

(21)). For mechanism (2) K°_p and K°_d values were negative in the region pH > 3.5, so that this assumption was disregarded as inadequate. Such finding was observed also when no charge separation within the surface complex was assumed. The results for mechanism (1) are presented in Fig. 5.

4.1.2. Calculation of thermodynamic adsorption equilibrium constant for mechanisms (1) and (2)

(vii) The values of the thermodynamic adsorption equilibrium constants K°_{a1} (for mechanism 1) and (for mechanism 2) were calculated from $\{\equiv$MOH$\}$ values (obtained in step v), experimental adsorption data (Γ_L) by applying DL approximation $\varphi_\beta = \varphi_d$ (φ_d values were obtained in step i). For mechanisms (1) and (2) the corresponding equations were used. Note that for mechanism (1): $\{\equiv$ML$^-\} = \Gamma_L$, while for mechanism (2) the similar relation holds: $\{(\equiv$M$)_2$L$^-\} = \Gamma_L$. It is interesting to note that despite the inadequate assumption (2) the adsorption equilibrium constant, as calculated for this mechanism, had reasonable value lg $K^\circ_{a2} = 12$. The results for mechanism (1) are presented in Fig. 6.

4.1.3. Calculation of inner layer capacitance C_1

(viii) The values of the surface charge density in 0-plane σ_0 were calculated from $\{\equiv$ MOH$_2^+\}$ and $\{\equiv$MO$^-\}$ values (obtained in step iv) and experimental Γ_L values. For mechanisms (1) and (2), Eqs. (17) and (18) were used, respectively. The calculated values depended on the assumed mechanism but did not depend on the choice of Γ_{tot}.

(ix) The values of inner layer capacitance C_1 were calculated from σ_0 values (obtained in step viii), measured φ_0 values and values of φ_β, approximated by φ_d (obtained in step i). The calculated values depended on the assumed mechanism but did not depend on the choice of Γ_{tot}. The results for mechanism (1) are presented in Fig. 9.

The values of the thermodynamic equilibrium constants for protonation (K°_p) and deprotonation (K°_d) of surface sites, as calculated by assuming mechanism (1), are presented in Fig. 5.
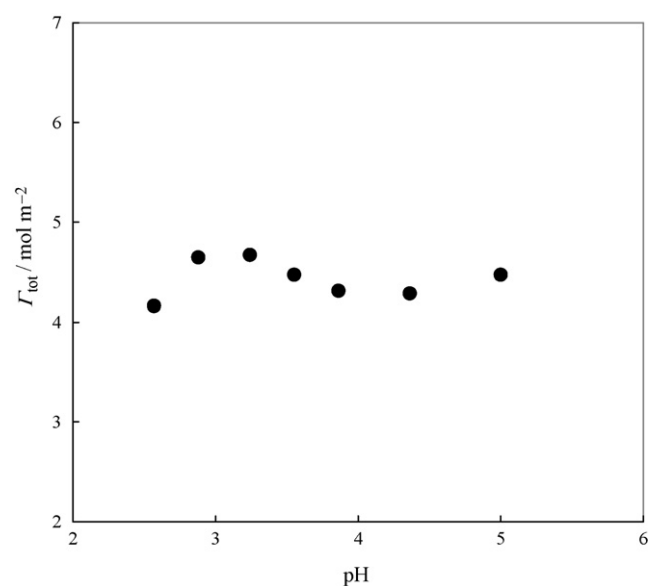

Fig. 7. Total density of surface sites calculated assuming 1-pK model.
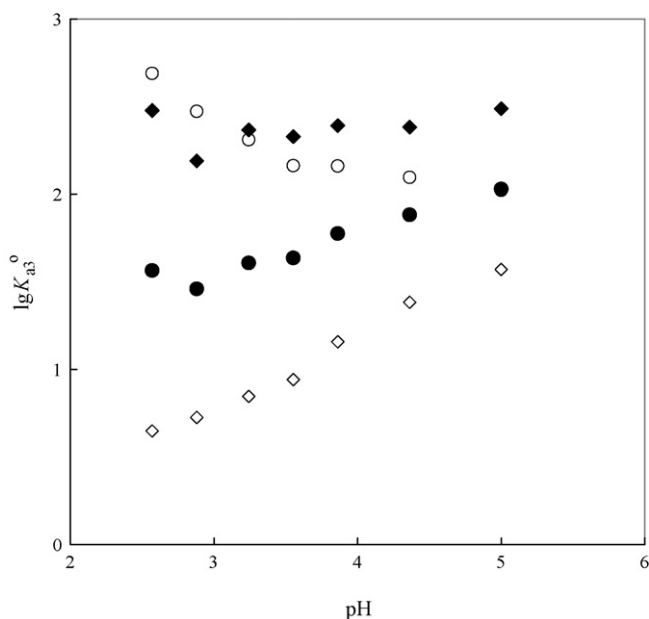
Fig. 8. Thermodynamic equilibrium constant of adsorption of salicylic acid at hematite, as calculated for 1-pK model using experimental data shown in Figs. 2–4. $I_c = 1.6 \times 10^{-2}$ mol dm^{-3}, $t = 25$ °C. Assumed value: $s = 10$ Å. The calculations were performed for different internal charge distributions within surface complex: $\equiv$M$^{1/2+}$L$^-$ (♦) and $\equiv$M$^+$L^{2-} (●). The corresponding results assuming that both ligand and metal are exposed to surface potential φ_0 are given by open symbols.

Mechanism (1) assumes binding of salicylate species to one surface metal atom through the oxygen bond. The values did not depend significantly on pH, but are still not quite constant in the examined pH range, which may be attributed to the experimental uncertainties. The choice of the electrokinetic slip plane sepa-
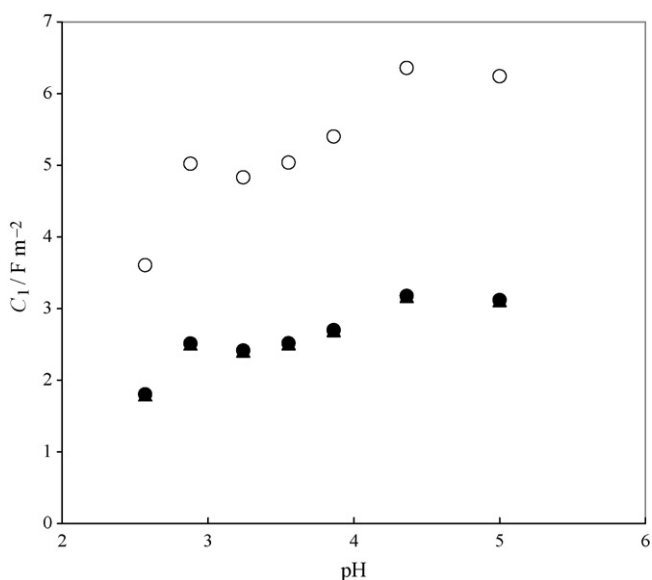

Fig. 9. Inner layer capacitance C_1 for the hematite/salicylic acid aqueous solution interface, as calculated for 2-pK and 1-pK models using experimental results shown in Figs. 2–4; $I_c = 1.6 \times 10^{-2}$ mol dm^{-3}, $t = 25$ °C. Assumed values: $\Gamma_{tot} = 1.5 \times 10^{-5}$ mol m^{-2}; $s = 10$ Å. In calculations different internal charge distributions within the surface complex were assumed: $\equiv$ML$^-$ (2-pK model ●), (1-pK model ▲) and $\equiv$M$^+$L^{2-} (2-pK model ○).

ration value did not significantly affect the result. The choice of the total density of surface sites would not affect the general feature. However, the higher Γ_{tot} values would produce higher values of both equilibrium constants [34].

A possible charge separation within the surface complex formed by mechanism (1), i.e. possible formation of $\equiv$M$^+$L^{2-} surface species was also tested. In that case K°_p and K°_d values did not change, while the adsorption equilibrium constant significantly decreased with pH.

4.2. The procedure for 1-pK mechanism is as follows

The procedure for 1-pK model is in principle similar to that described for 2-pK model of surface reaction but differs in several points:

(x) Calculation of φ_d and σ_s from ζ-potentials is the same as in case of 2-pK model.

(xi) Calculation of the ratio of positive and negative surface sites $\{\equiv$MOH$^{1/2+}\}/\{\equiv$MO$^{1/2-}\}$ from Eq. (28) is similar to the calculation shown in step iii.

(xii) Individual values of $\{\equiv$MOH$^{2+}\}$ and $\{\equiv$MO$^{1/2-}\}$ were obtained from σ_s (in step x) and their ratio using

$$\sigma_s = F(0.5\{\equiv \text{MOH}^{1/2+}\}$$
$$-0.5\{\equiv \text{MO}^{1/2-}\} - 0.5\{\equiv \text{M}^{1/2+}\text{L}^{1-}\}) \qquad (30)$$

by taking $\{\equiv$M$^{1/2+}$L$^{1-}\} = \Gamma_L$.

(xiii) The total density of 1-pK surface sites was calculated using individual values for charged surface sites (obtained in step xii) and the adsorption data for salicylic acid

$$\Gamma_{tot} = \{\equiv \text{MOH}^{1/2+}\} + \{\equiv \text{MO}^{1/2-}\} + \Gamma_L \qquad (31)$$

Results are presented in Fig. 7.

(xiv) The equilibrium constant of adsorption of salicylic acid on hematite, K°_{a3}, was calculated on the basis of Eq. (24) using individual values of $\{\equiv$MOH$^{1/2+}\}$ (obtained in step xii) and adsorption data $\{\equiv$M$^{1/2+}$L$^{1-}\} = \Gamma_L$. In calculations the φ_β and values were used as obtained previously (step x). Results for different assumed charge distributions within surface complex are presented in Fig. 8

(xv) The capacitance of the inner layer C_1 was calculated as in step ix by taking:

$$\sigma_0 = F(0.5\{\equiv \text{MOH}^{1/2+}\} - 0.5\{\equiv \text{MO}^{1/2-}\}$$
$$+0.5\{\equiv \text{M}^{1/2+}\text{L}^{1-}\}) \qquad (32)$$

The results for both 2-pK and 1-pK models are presented in Fig. 9.

The analysis based on 1-pK mechanism showed a very good agreement between the model and the experimental data. At first, the protonation thermodynamic equilibrium constant $K^\circ_{1/2}$ did not depend on pH, which is due to the definition (29). The thermodynamic equilibrium constant of adsorption was found to be independent on pH for the $\equiv$M$^{1/2+}$L^{1-} conformation. Other possibilities of charge distribution within the surface complex

did not result in the constancy of the adsorption equilibrium constant.

The capacitance of the inner layer was found to be same for 2-pK and 1-pK mechanisms. The total density of surface sites was found to be practicality independent on pH, which supports the proposed interpretation. The obtained value of $\Gamma_{tot} = 4.5 \times 10^{-6}$ mol m^{-2} is reasonable.

5. Discussion

Results presented in this article could be considered semi quantitatively but on higher level they could also be interpreted quantitatively. In the presence of salicylic acid, the isoelectric point is shifted to acidic region, which indicates the formation of negatively charged surface species (Fig. 3). The point of zero potential practically remains the same, which means that negative charges are not formed in the inner 0-plane (Fig. 2). The adsorption isotherm shows a maximum at approximately pH 3, which is due to the interplay of two phenomena (Fig. 4). At lower pH values the surface is more positively charged increasing the attraction of negative species from the bulk of the solution. However, at pH < 4 the fraction of negatively charged HL$^-$ species in the solution decreases (Fig. 4). Formation of the complex with two neighboring surface metal ions leads to uncharged complex, and is thus not probable. The interpretation was performed using both 2-pK and 1-pK models of surface charging. Both models agreed with experimental data leading to the same conclusion that salicylic acid is bound to one metal through two oxygen bounds. Quantitative analysis provides values of the equilibrium parameters. For 2-pK model, assumption that salicylic acid is bound to two surface metal atoms led to negative values of K°_p and K°_d in the region pH > 3.5, so that this assumption should be disregarded. However, assuming the binding with one surface metal atom the positive and reasonably constant K°_p and K°_d values were obtained (Fig. 5). Also, the thermodynamic adsorption equilibrium constant K°_{a1} was found to be practically independent on pH, as required (Fig. 6). The mechanism (1) allows the assumption of internal charge separation within the surface complex. The stoichiometry and total charge remains the same if, e.g. $\equiv M^+ L^{2-}$ surface complex is formed. The only difference lies in the activity coefficient due to the electrostatic effects since the metal is exposed to surface potential φ_0, while the organic part is exposed to φ_β. This possibility was examined; the K°_p and K°_d values remained the same, while K°_{a2} values were higher and decreased with pH (Fig. 6). The effect of charge separation was tested also for mechanism (2) but again no reasonable results were obtained. Interpretation based on 1-pK model shows the agreement with experimental data if the formation of $\equiv M^{1/2+} L^{1-}$ complex is assumed. The conclusion is based on the pH independency of thermodynamic equilibrium constant of adsorption and of the value of Γ_{tot}. Results of this study suggest that a surface salicylate complex with one Fe atom at the hematite surface with total charge -1 is formed. This conclusion is based on the interpretation based on both 1-pK and 2-pK mechanisms. The examined data did not provide information on the type of the bond; both monodentate and bidentate complex might be formed. However, IR and Raman spectroscopy showed
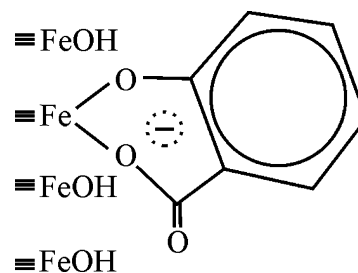

Fig. 10. The conformation of salicylate complex at the hematite surface.

that Fe in solid state strongly and simultaneously interacts with carboxylate and hydroxyl of salicylic molecule [35]. Based on the interpretation presented in this article and the spectroscopy data one may conclude that the salicylate ions are bound to Fe at the surface through two oxygen bonds, as shown in Fig. 10.

In Fig. 9, calculated values of the inner layer capacitance C_1 for 2-pK model (mechanism 1), assuming also the charge separation within the surface complex, are displayed. The same values were obtained for 1-pK model. The values are reasonable and increase with pH, which does not contradict to the model since the constancy of C_1 is not required [36,37]. In the interpretation, the value of electrokinetic slip plane separation s was assumed. Also for 2-pK model it was necessary to assume the value of total concentration of surface sites Γ_{tot}. While the choice of the s value did not significantly affect the results, the values of equilibrium parameters are dependent on Γ_{tot}. However, the general feature remained the same supporting the above conclusion on the conformation of the surface complex.

References

[1] R. Kummert, W. Stumm, J. Colloid Interface Sci. 75 (1980) 373–385.
[2] Y. Zhang, N. Kallay, E. Matijević, Langmuir 1 (1985) 201–206.
[3] N. Kallay, E. Matijević, Langmuir 1 (1985) 195–201.
[4] A.E. Regazzoni, M.A. Blesa, A.J.G. Maroto, J. Colloid Interface Sci. 122 (1988) 315–325.
[5] R. Torres, N. Kallay, E. Matijević, Langmuir 14 (1988) 706–710.
[6] M.V. Biber, W. Stumm, Environ. Sci. Technol. 28 (1994) 763–768.
[7] J.D. Filius, T. Hiemstra, W.H. Van Riemsdijk, J. Colloid Interface Sci. 195 (1997) 368–380.
[8] D. Kovačević, N. Kallay, I. Antol, A. Pohlmeier, H. Lewandowski, H.D. Narres, Colloids Surf. A 140 (1998) 261–267.
[9] A.E. Regazzoni, P. Mandelbaum, M. Matsuyoshi, S. Schiller, S.A. Bilmes, M.A. Blesa, Langmuir 14 (1998) 868–874.
[10] D. Kovačević, I. Kobal, N. Kallay, Croat. Chem. Acta. 71 (1998) 1139–1153.
[11] C.R. Evanko, D.A. Dzombak, J. Colloid Interface Sci. 214 (1999) 189–206.
[12] M.A. Blesa, A.D. Weisz, P.J. Morando, J.A. Salfity, G.E. Magaz, A.E. Regazzoni, Coord. Chem. Rev. 196 (2000) 31–63.
[13] O.W. Duckworth, S.T. Martin, Geochim. Cosmochim. Acta 65 (2001) 4289–4301.
[14] A.D. Weisz, A.E. Regazzoni, M.A. Blesa, Solid State Ionics 143 (2001) 125–130.
[15] A.D. Weisz, L.G. Rodenas, P.J. Morando, A.E. Regazzoni, M.A. Blesa, Catal. Today 76 (2002) 103–112.
[16] J. Rosenqvist, K. Axe, S. Sjöberg, P. Persson, Colloids Surf. A 220 (2003) 91–104.
[17] S.B. Johnson, T.H. Yoon, A.J. Slowey, G.E. Brown, Langmuir 20 (2004) 11480–11492.
[18] M.R. Das, D. Bordoloi, P.C. Borthakur, S. Mahiuddin, Colloids Surf. A 254 (2005) 49–55.

[19] S.J. Hug, D. Bahnemann, J. Electron. Spectrosc. Relat. Phenom. 150 (2006) 208–219.

[20] T. Lana-Villarreal, J.M. Pérez, R. Goméz, C. R. Chem. 9 (2006) 806–816.

[21] L. Ojamäe, C. Aulin, H. Pedersen, P.-O. Käll, J. Colloid Interface Sci. 296 (2006) 71–78.

[22] T. Zuyi, C. Tawei, J. Colloid Interface Sci. 231 (2000) 8–12.

[23] E. Yates, S. Levine, T.W. Healy, J. Chem. Soc. Faraday Trans. I 70 (1974) 1807–1818.

[24] T. Hiemstra, W.H. van Riemsdijk, G.H. Bolt, J. Colloid Interface Sci. 133 (1989) 91–104.

[25] N. Kallay, Z. Dojnović, A. Čop, J. Colloid Interface Sci. 286 (2005) 610–614.

[26] N. Kallay, D. Kovačević, A. Čop, in: N. Kallay (Ed.), Interfacial Dynamics, Marcel Dekker, Inc., New York, 2000.

[27] N. Kallay, S. Žalac, J. Colloid Interface Sci. 230 (2000) 1–11.

[28] N. Kallay, T. Preočanin, S. Žalac, Langmuir 20 (2004) 2986–2988.

[29] G.A. Parks, Chem. Rev. 65 (1965) 177–198.

[30] N. Kallay, A. Čop, T. Preočanin, D. Kovačević, Ann. UMCS 60 (2005) 47–64.

[31] M.A. Pyman, J.W. Bowden, A.M. Posner, Aust. J. Soil Res. 17 (1979) 191–195.

[32] J. Lützenkirchen, P. Magnico, Colloids Surf. A 137 (1998) 345–354.

[33] T. Preočanin, N. Kallay, A. Čop, J. Colloid Interface Sci. 299 (2006) 772–776.

[34] K.F. Hayes, G. Redden, W. Ela, J.O. Leckie, J. Colloid Interface Sci. 142 (1991) 448–469.

[35] M.C. Alvarez-Ros, S. Sanchez-Cortes, J.V. Gracia-Ramos, Spectrochim. Acta A 56 (2000) 2471–2477.

[36] N. Kallay, D. Kovačević, A. Čop, M. Medvidović, Croat. Chem. Acta 77 (2004) 243–249.

[37] T. Preočanin, W. Janusz, N. Kallay, Evaluation of equilibrium parameters of the anatase/aqueous electrolyte solution interface by introducing surface potential data, Colloids Surf. A: Physicochem. Eng. Aspects 297 (2007) 30–37.

[38] The IUPAC Stability Constant Database, Academic Software and IUPAC, 1992–2000.